Pergamon

Bioorganic & Medicinal Chemistry 9 (2001) 2745–2756

BIOORGANIC & MEDICINAL CHEMISTRY

Design and Structure–Activity Relationship of Thrombin Inhibitors with an Azaphenylalanine Scaffold: Potency and Selectivity Enhancements Via P2 Optimization

A. Zega,[a] G. Mlinšek,[b] P. Šepic,[a] S. Golič Grdadolnik,[b] T. Šolmajer,[b,c] T.B. Tschopp,[d] B. Steiner,[d] D. Kikelj[a] and U. Urleb[a,c,*]

[a]*Faculty of Pharmacy, University of Ljubljana, Aškerčeva 7, 1000 Ljubljana, Slovenia*
[b]*National Institute of Chemistry, POB 3430, Hajdrihova 19, 1115 Ljubljana, Slovenia*
[c]*Lek, d.d., Pharmaceutical and Chemical Company, 1526 Ljubljana, Slovenia*
[d]*Pharma Division, Preclinical Research, F. Hoffmann La Roche Ltd, 4002 Basel, Switzerland*

This paper is dedicated to Professor Dr. M. Tišler (Ljubljana) in honor of his 75th birthday

Received 6 February 2001; accepted 15 June 2001

Abstract—Theoretical and structural studies followed by the directed synthesis and in vitro biological tests lead us to novel non-covalent thrombin pseudopeptide inhibitors. We have incorporated an azapeptide scaffold into the central part of the classical tripeptide D-Phe-Pro-Arg inhibitor structure thus eliminating one stereogenic center from the molecule. A series of compounds has been designed to optimize the occupancy of the S2 pocket of thrombin. Increased hydrophobicity at P2 provides an enhanced fit into this active site S2 pocket. In the present paper, we also report on the structure of these inhibitors in solution and conformational analysis of inhibitors in the active site in order to asses the consequences of the replacement of the central α-CH by a nitrogen functionality. In vitro biological testing of the designed inhibitors shows that elimination of *R, S* stereoisomerism and restriction of conformational freedom influences the binding of inhibitors in a favorable fashion.

Introduction

Thrombin is a trypsin-like serine protease that plays a central role in the blood coagulation process. It cleaves and thus transforms fibrinogen to insoluble fibrin which is the major component of a blood clot.[1] Unbalanced hemostasis can lead to arterial and venous thrombosis which are important causes of morbidity and mortality. An effective, especially orally active, thrombin inhibitor that would cause fewer side effects than the currently used heparin and warfarin would therefore be of clinical importance.[2,3]

Thrombin inhibitors are intensively sought after worldwide. A therapeutically useful protease inhibitor should be potent, selective and orally bioavailable. The best studied inhibitors are derived from the sequence D-Phe-Pro-Arg as found in the clinically used compound Argatroban (**1**, Novastan). However, the strong basicity of the P1 residue of these inhibitors which are completely protonated under all physiologcal conditions hamper the passive diffusion across intestinal barriers that is the main route of absorption for most drugs.[4–17] Closely related derivatives of Argatroban, such as the amidrazone derivative LB-30,057[18–20] (**2**) and the benzamidine derivative UK 156,406[21] (**3**) have recently been identified as orally active thrombin inhibitors (Fig. 1).

Replacement of the strongly basic groups in potent thrombin inhibitors by less basic ones is usually accompanied by a decreased potency.[9,10] Thus, a compromise is being sought in order to simultaneously obtain sufficient affinity, selectivity and bioavailability. In this paper, we present a novel series of noncovalent inhibitors which have been optimized for reduced basicity at the S1 pocket and contain a conformationally restricted substituent aimed at the S2 binding pocket in the active site of thrombin (Fig. 2).

Azaamino acids are important constituents of pseudopeptides and are particulary important as protease inhibitors and inhibitors of other enzymes.[22–27] Replacement

*Corresponding author. Tel.: +386-1-476-9500; fax: +386-1-425-8031; e-mail: urlebu@ffa.uni-lj.si

0968-0896/01/$ - see front matter
PII: S0968-0896(01)00202-4

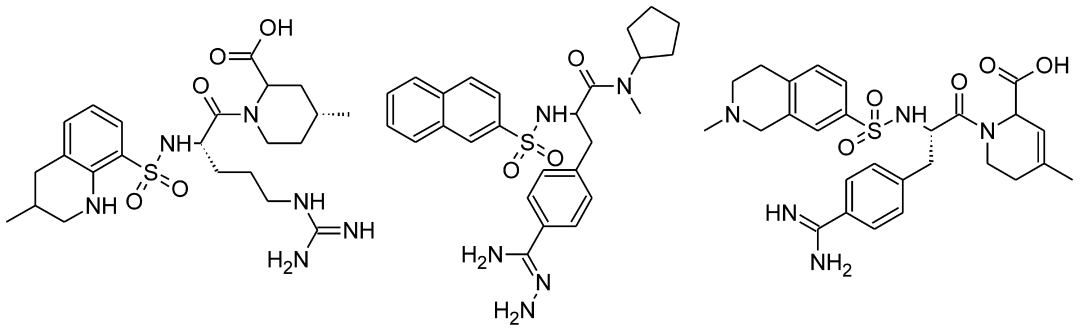

Figure 1. Structures of thrombin inhibitors.

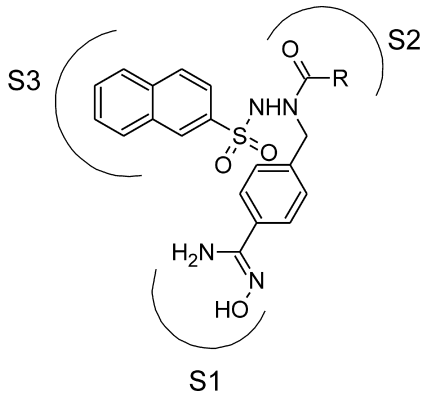

Figure 2. Schematic drawing of the thrombin inhibitor in the active site of thrombin (R moieties are defined in Table 4).

of the central α-CH of the amino acid residue by nitrogen has little effect on the overall polarity of the molecule but would be expected to provide for novel chemical and biological properties, by virtue of reduced conformational flexibility. The incorporation of an azapeptide scaffold into the argatroban-like thrombin inhibitor structure[9] was expected to be beneficial for two reasons. Firstly, the change in the overall conformation might lead to higher affinity for the binding site. Secondly, the resulting compound might be more stable to enzymatic degradation and thus have longer duration of action.[22,28] In addition, the absorption and transport properties might be favorably altered.

We have performed both a careful molecular modeling study in the thrombin active site based on published X-ray structures of various inhibitor–thrombin complexes, and a structural study of inhibitors in solution using 2-D NMR spectroscopy to explore how these changes alter the hydrophobic and electrostatic interactions with the enzyme.

Results and Discussion

Chemistry

All target compounds shown in Table 1 were prepared according to Scheme 1.

Commercially available 4-cyanobenzaldehyde **1** was transformed into the corresponding hydrazone **2** using *tert*-butylcarbazate followed by catalytic hydrogenation on Pd/carbon to give intermediate **3**. Coupling of this aryl tert-butyl hydrazinecarboxylate with cyclic amines yielded the required Boc protected carbazamides **4a**–**d** in a one-pot synthesis utilizing commercially available triphosgene. Deprotecting the Boc group in compounds **4a**–**d** by treatment with gaseous HCl in AcOH and subsequent reaction with naphthalene-2-sulfonylchloride led to compounds **5a**–**d**. Finally, hydroxylamine was used to convert the nitriles **5a**–**d** to the target benzamidoximes **6a**–**d**.

With the N^{α}-substituted-N^{β}-protected hydrazines triphosgene gives the corresponding carbazic acid chlorides in situ which cannot be isolated. These react rapidly at low temperature with the amine to yield N^{β} protected carbazamide.[29]

Solution structures determined by 2D NMR

The proton chemical shifts assignment and proton–proton distance determination of **6a**–**d** were determined following standard procedures, that is homonuclear DQF-COSY, TOCSY, and NOESY experiments.

The experimentally derived distances were incorporated as conformational restraints in extensive molecular dynamics simulations carried out in explicit DMSO.[30] By the application of the force field used in the molecular dynamics simulations, important energetic features of the molecule are included in the analysis. Moreover, the inclusion of explicit solvent molecules improves the energetic refinement given the large surface area of the molecules.

Even with different starting structures, the molecular dynamics (MD) simulations of all compounds always resulted in large Nuclear Overhauser Enhacement (NOE) violations: sometimes with violations as high as 1.5 Å. This is an indication that the experimental constraints cannot be satisfied by a single conformation. Therefore we carried out MD simulations with different sets of experimental constraints. After careful examination of distance violations we found that there are four main groups of conformations which differ from one another in the orientation of the naphthalene, the

Table 1. Conformational constraints (Å) of compounds **6a–d** determined from NOESY or ROESY spectra and distance violations (Å) from restrained simulations

Conformational constraints	**6a**							**6b**		**6c**		**6d**	
	Conf.:	a	b	c	d	e	f	Conf. A		Conf. A		Conf. A	
	Dist.	Viol.	Viol.	Viol.	Viol.	Viol.	Viol.	Dist.	Viol.	Dist.	Viol.	Dist.	Viol.
Pip-H^2–H^3												2.410	0.02
Pip-$H^{2'}$–H^3								2.325	0.00				
Pip-$H^{2'}$–$H^{3'}$								2.424	0.00			2.339	0.07
Pip-H^6–H^7												2.410	0.00
Pip-$H^{5'}$($H^{6'}$) –$H^{6'}$($H^{7'}$)								2.569	0.00			2.339	0.01
CH_3–Pip-$H^{2'}$								2.805	0.05				
CH_3–Pip-$H^{3'}$								3.060	0.00				
CH_3–Pip-H^4								3.245	0.01				
CH_3–Pip-H^6								3.730	0.13				
Pip-H^6–H^4								2.581	0.04				
Pip-H^6–$H^{5'}$								2.424	0.00				
Pip-H^6(H^7) –NH	3.949	0.39	0.25							3.448	0.11	3.257	0.21
Pip-$H^{6'}$–NH								3.942	0.33				
Pip-H^6(H^7)–$CH_2$1	3.138	0.13	0.17									3.054	0.12
Pip-H^6(H^7)–$CH_2$2	2.555	0.31	0.29									2.993	0.21
Pip-$H^{6'}$–$CH_2$1										2.789	0.03		
Pip-$H^{2'}$–$CH_2$1				0.27	0.29								
Pip-$H^{2'}$–$CH_2$2				0.25	0.27								
Pip-$H^{2'}$–NH				0.30	0.29								
Nph-H^1–Pip-$H^{2'}$				0.13									
Nph-H^1–NH	3.333	0.10		0.18		0.12		3.835	0.11	3.100	0.23	3.137	0.13
Nph-H^1–Pip-H^6(H^7)	3.787	0.11						3.322	0.18	3.543	0.11	3.540	0.16
Nph-H^1–Pip-$H^{6'}$								2.920	0.13				
Nph-H^1–Pip-$H^{4,4'}$(H^5)	4.839	0.09		0.07		0.08						3.579	0.15
Nph-H^1–CH_3										6.240	0.10		
Nph-H^1–$CH_2$1	4.031						0.39						
Nph-H^3–NH	2.836		0.36		0.34		0.43						
Nph-H^3–Pip-$H^{2'}$					0.13								
Nph-H^3–Pip-H^6	4.103		0.15										
Nph-H^3–$CH_2$1	4.301					0.29							
Nph-H^4–Pip-$H^{4,4'}$	5.050		0.09		0.13		0.18						
Nph-H^4–Pip-$H^{2'}$					0.25								
Nph-H^8–Pip-$H^{4,4'}$(H^5)	4.410	0.11		0.16		0.27						3.557	0.16
Nph-H^8–Pip-H^6	4.320	0.47						3.143	0.24				
Pip-H^8–Pip-$H^{6'}$								4.239	0.15				
Nph-H^8–CH_3										4.625	0.16		
Nph-H^8–Pip-$H^{2'}$				0.19									
NH–$CH_2$1	3.256	0.05	0.05	0.06	0.06	0.07	0.05					3.183	0.31
NH–$CH_2$2												3.230	0.35
Ar-H^2–Pip-H^2				0.34	0.38								
Ar-H^2–Pip-$H^{2'}$								4.025	0.13				
Ar-H^2–Pip-$H^{6'}$($H^{7'}$)	4.000	0.27	0.35							3.963	0.30	3.966	0.27
Ar-H^2–$CH_2$1	2.868	0.12	0.10	0.10	0.08					2.879	0.12	3.271	0.45
Ar-H^6–$CH_2$2	2.896	0.08	0.09	0.11	0.10			2.849	0.07	2.875	0.07	3.368	0.32
Ar-H^2–$CH_2$2	2.896					0.13	0.07						
Ar-H^6–$CH_2$1	2.868					0.06	0.11						
Ar-H^6–NH	3.415	0.12	0.14	0.10		0.10	0.14	3.412	0.12	3.395	0.15	3.341	0.16
Ar-$H^{2,6}$–NH_2										5.369	0.00		
Ar-$H^{3,5}$–NH_2	2.844	0.00	0.00	0.00	0.00	0.00	0.00			2.777	0.00		
Ar-$H^{3,5}$–OH	4.257	0.24	0.24	0.19	0.35	0.25	0.26						
OH–NH_2	3.858	0.32	0.36	0.33	0.30	0.34	0.29						
Average violation		0.18	0.19	0.17	0.21	0.16	0.19		0.09		0.11		0.17

piperidine or hexahydro-1H-azepin ring and the benzamidoxime spacer CH_2 group (Fig. 3a and b). When only NOEs which are consistent with a particular orientation of the above-mentioned groups were included in MD simulations, the resulting structures had low average distance restraint violations between 0.1 and 0.2 Å and all NOE violations were less than 0.5 Å (Table 1).

The different orientation of the above-mentioned rings and the CH_2 group do not significantly influence the overall conformation of **6a** (Fig. 3a). Therefore, since we were interested in the influence of different substituents on the conformation of molecules only simulations with one particular orientation of flexible groups were performed for the other molecules (**6b–c**) (Fig. 3b). The resulting conformations of analogues are similar and have a typical Y-conformation. The piperidine and naphthalene rings are forming the upper part of Y while the benzamidoxime moiety is perpendicular to the other two rings forming the lower part of Y. Analogue **6b** is an exception, it has a perpendicular orientation of the piperidine and naphthalene rings.

Solution conformations of the molecules do not change significantly after their energy minima were determined in the thrombin active site (Fig. 3a and b).

Conformational search by systematic rotations

Based on the X-ray structure of the complex of thrombin inhibitor BMS 189,090[31] with thrombin and the solution structure of *N*′-hydroxy-4-{[2-(2-naphtylsulfonyl)-1-(1-piperidinylcarbonyl)hydrazino]methyl} benzenecarboximidamide (**6a**), we analysed the flexibility of the ligands in the active site of thrombin in order to gather information on their binding properties.

We have chosen BMS 189,090 for comparison since it has a low affinity constant ($K_i = 3.6$ nM) and a 3-D structure similar to the solution structure of **6a** [the root mean square deviation (RMS) obtained from superposition of 40 common heavy atoms of the two compounds is 1.3 Å]. Partial conformational analysis was performed by rotating parts of the inhibitor molecule around selected flexible bonds. Flexible bonds were

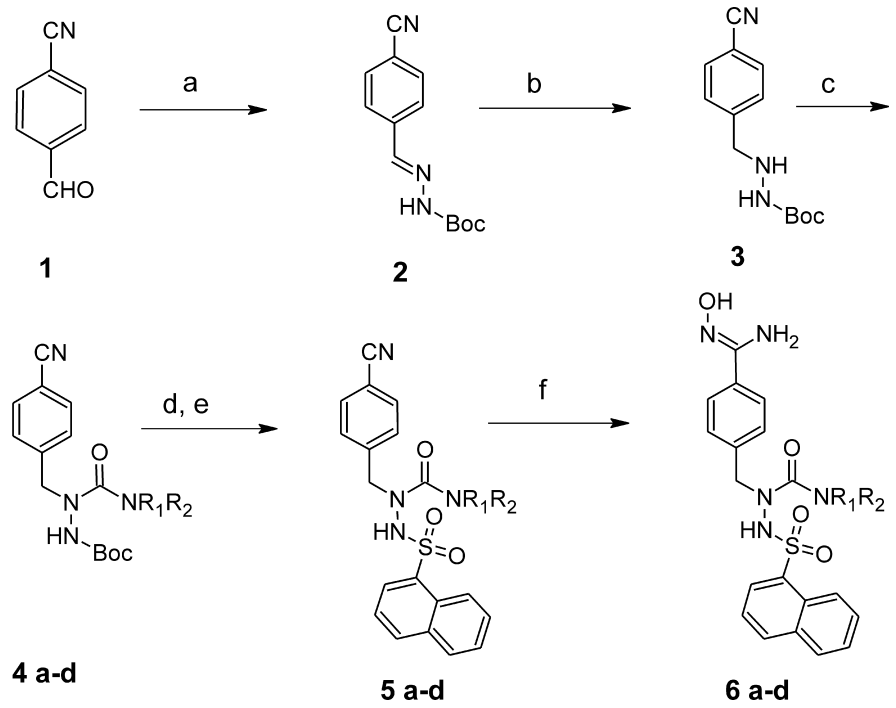

Scheme 1. (a) Boc-$NHNH_2$, EtOH, reflux, 95%; (b) H_2, Pd/C, MeOH, 97%; (c) (1) $(Cl_3CO)_2CO$, CH_2Cl_2, (2) HNR^1R^2, DIEA, 35–81%; (d) HCl (g), AcOH; (e) naphtalene-2-sulfonyl chloride, CH_2Cl_2, Et_3N, 22–33%; (f) NH_2OH, EtOH, reflux, 38–57%.

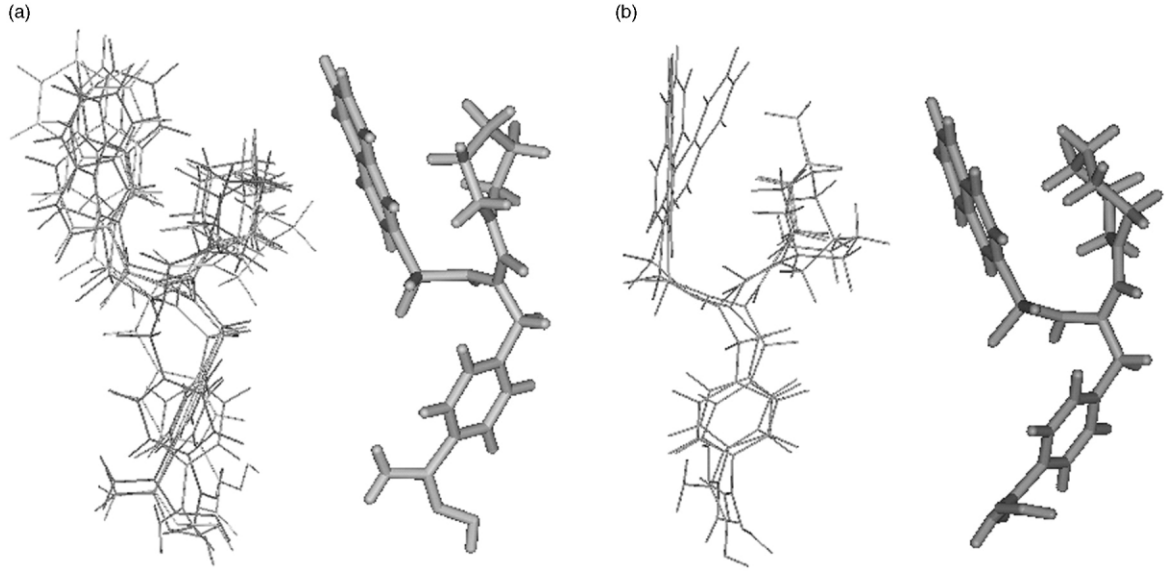

Figure 3. (a) Comparison of solution conformations of **6a** (thin lines) with the conformation of **6a** (heavy lines) as modeled in the thrombin active site. The various orientations of the naphthalene, piperidine ring and benzamidoxime are shown. (b) Comparison of solution conformations of **6b–c** (thin lines) with the structure of **6a** (heavy lines). The various orientations of the naphthalene, piperidine and benzamidoxime moiety are shown.

defined as given in Fig. 4 and a total of two single dihedral angle rotations and three coupled dihedral angle rotations were performed. These rotations were chosen as a reasonable compromise between the combinatorial blow up in the case of a systematic conformational analysis for all eight bonds (360/10**8 rotational conformers) and taking into account the Y structure of the inhibitor molecule. The resulting conformations were compared and possible reasons for the different binding affinities were elucidated.

The following structural properties were addressed by in our series of ligands: the role of the central nitrogen atom in **6a–d**, the effect of the addition of a CH_3 group to the piperidine ring and the replacement of the piperidine ring by a seven-membered ring. A general result observed from the data in Table 2 is that in the case of coupled dihedral angle rotations only a small fraction (5–10%) of the conformations are accessible. From this we can deduce that the inhibitor fits reasonably well into all three active site pockets S1–S3 of the enzyme. Furthermore, the position and size of substituent at S2 influences the number of possible energetically favorable conformers. Flexibility of the piperidinyl carbonyl substituent is much smaller than for the benzamidoxime. This can be atributed to the flexible methylene group connecting the benzamidoxime ring with the central nitrogen atom.

In the case of single dihedral angle α1 which defines the rotations of amidoxime functionality found, nearly all available conformers (between 65 and 71 out of a possible 72) are possible. This is drastically different from rotations about angle α0 which defines the rotations of the P2 moiety where only between 9 and 17 conformers are available in the inhibitors (Fig. 5a and b). This finding can be further elaborated: in the case of angle α4 which distinguishes between the central N and the α-CH, the possible number of accessible conformers is significantly larger for nitrogen. Thus, releasing of the stereoisomer constraint by having nitrogen on the planar aza skeletal element enhances the possibility that the inhibitor ligand will fit into the active site pocket.

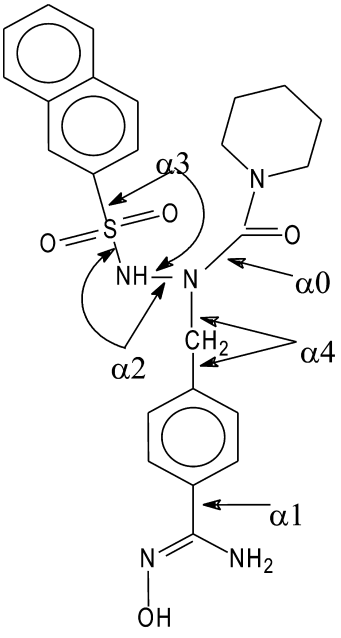

Figure 4. Torsion angles definitions in molecules **6a–d**.

Our initial hypothesis based on the study of model peptides containing aza aminoacids was that the central nitrogen atom influences surrounding bonds and makes them more rigid. Whether the introduction of a rigid structural element favors the complexation of the inhibitor with the target protein was determined by comparison of identical inhibitors differing only in that the central α-CH was substituted by nitrogen. Previous work done by Bode et al.[32] shows the importance of *R, S* stereoisomerism in α-CH analogues. Since the free electron pair of nitrogen means that the molecule has no chiral properties compared to chiral α-CH carbon atom this substitution should facilitate the more favorable 'planar configuration' of the inhibitor in the protein. Data obtained through systematic conformational search show that the dihedral α2 of the studied inhibitors has only roughly half of the favorable conformations observed for the rotation of dihedral α4. There are several possible explanations for this. One might be that the rigidity introduced by the nitrogen atom acts as a barrier to rotation thus precluding successful adaptation of dihedrals to the furrowed surface of the thrombin active site and increasing fluctuations. Another possible explanation is the planarity around the central N atom compared to the C atom. It could also be that the backbone of the inhibitor gets displaced due to the higher electronegativity of the N compared to the C atom although a direct hydrogen bond between the central N atom and surrounding residues was not observed in our simulations (Table 3).

The distal part of the ligands projecting into the S3 pocket (2-naphthalenesulfonylhydrazide) is much less flexible than the central part of the molecule around the N–N bond. This can be attributed to the tight fit of the ligand into the active site via multiple hydophobic and steric contact points at this part of the inhibitor surface. The *ortho* (structure **6bC**) and *para* (structure **6cC**) methyl substituent of the piperidine ring it is limiting the α-CH analogues much less than the nitrogen analogues **6b** and **6c**.

This is further corroborated by data presented in Table 3.

Table 2. The total number of favorable conformations of inhibitors **6a–d** and their carbon analogues as obtained by rotations around dihedrals in active site of thrombin (dihedral angles are defined in Fig. 4). The number of favorable conformations in all potential minima are also included

Compd	α0	α1	α2	α3	α4
6a	12	66	36	71	131
6aC	10	69	25	80	94
6b	9	67	13	50	98
6bC	9	66	25	49	86
6c	17	71	14	53	102
6cC	11	68	27	53	88
6d	13	66	39	60	118
6dC	15	65	13	48	98

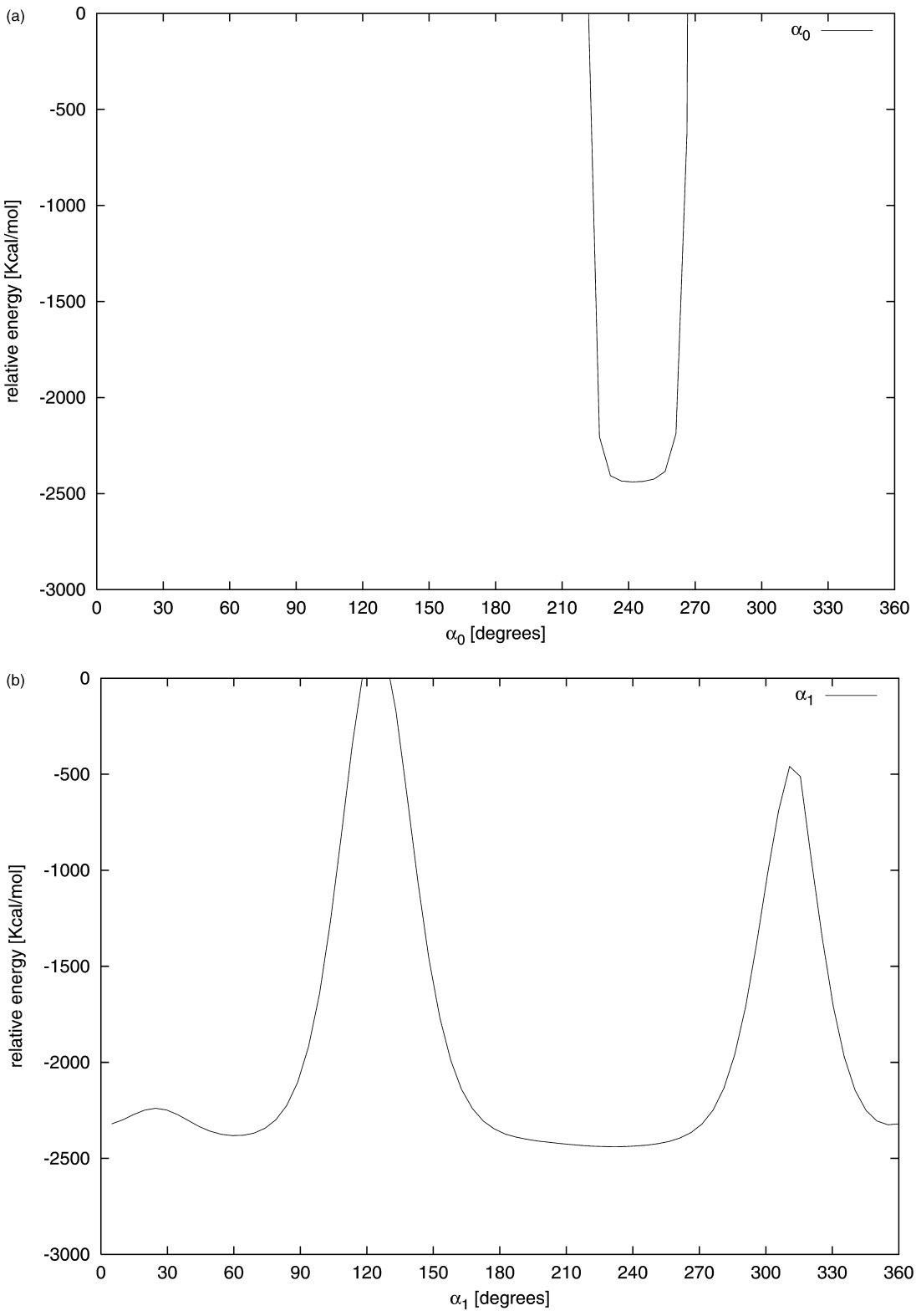

Figure 5. (a) Relative energy profiles for conformational dependence of the inhibitor–thrombin complex on α0. (b) Relative energy profiles for conformational dependence of the inhibitor–thrombin complex on α1.

The hydrogen bonds observed for the aza analogues in the thrombin active site are as expected. It may be of importance for the interpretation of the inhibitory activity of methyl substituted P2 moieties that for these molecules there are more H bonds (5 and 4) than for the unsubstituted analogue **6a** (2).

The most important difference in the active site of thrombin compared with that of trypsin is the YPPW loop (Tyr60a–Trp60d) which serves to bind small lipophylic groups in thrombin but is absent in trypsin. We therefore expected to see an increased binding of the substituted piperidine moiety to the thrombin S2

pocket. We found that the increased number of conformers for dihedral angle α0 of the *para* methyl substituted N analogue **6c** favorably influences the binding activity when compared with the carbon analogue **6cC**.

Biological evaluation

The in vitro data for the series **6a–d** are summarized in Table 4. Chromogenic assays were performed with standard set of serine proteases from thrombin family including thrombin, fXa, fVIIa and trypsin. The selectivity ratio of trypsin/thrombin is given in Table 4.

Introduction of a nitrogen funcionality into the central part of the inhibitor series has had a favorable effect on binding. Compound **6d** ($K_i = 0.201\ \mu M$) exhibited 6-fold potency enhancement over the corresponding α-CH analogue ($K_i = 1.140\ \mu M$).[18]

We have focused our attention principally on the S2 pocket. Methylation and enlargement of the piperidine ring resulted in increased hydrophobicity at the P2 part of the molecule, resulting in a 10-fold increase in **6d** potency compared to **6a**.

The pK_a values of benzamidoxime, that is a pK_{a_1} of approximately 13 (deprotonation) and a pK_{a_2} of approximately 5 (protonation), indicate that our compounds remain uncharged over a wide pH range. This property could enhance oral absorption.[33]

Table 3. Hydrogen bonds between inhibitors and thrombin residues

Compd	Number of H bonds	Distance (Å)	Angle (°)	Residue	Compd atom
6a	1	2.08	165.95	cys 191 N	N1 (amide)
	2	2.49	138.91	gly 216 N	N (oxime)
6b	1	2.44	144.82	glu 192 OE1	N1 (amide)
	2	2.22	138.35	ser 195 OG	N1 (oxime)
	3	2.36	175.29	gly 216 N	N1 (oxime)
	4	1.67	168.26	ala 190 O	OH (oxime)
	5	1.99	164.09	ala 190 O	N1 (amide)
6c	1	2.25	151.83	gly 216 N	O3 (sulphur)
	2	2.12	160.14	gly 219 O	N1 (amide)
	3	1.58	167.30	asp 189 OD2	OH (oxime)
	4	1.88	165.82	asp 189 OD2	N1 (oxime)
6d	1	2.05	137.51	asp 189 OD2	N1 (amide)
	2	2.46	154.82	asp 221 N	O3 (oxime)
	3	1.63	175.06	ala 190 O	O3 (oxime)

Table 4. Structure–activity relationship of P2 directed aza inhibitors

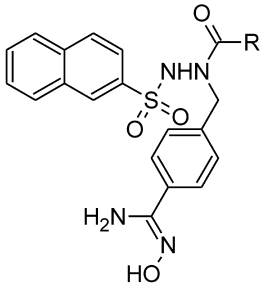

Compd	R	K_i (μM)				
		Thr	fXa	fVIIa	Tryp	Tryp/Thr
6a	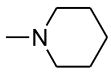	1.938	> 69.4	> 75.4	> 68.3	> 35.2
6b	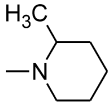	0.427	> 69.4	> 75.4	45.308	107.8
6c	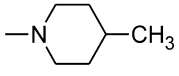	0.768	> 69.4	> 75.4	> 68.3	> 88.9
6d	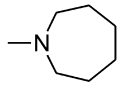	0.201	> 69.4	> 75.4	13.341	66.5

Conclusion

By using a structure-based approach to design novel thrombin inhibitors, we developed a novel class of direct noncovalent inhibitors with moderate affinities for thrombin and good selectivity over trypsin. The main characteristic of our compounds is the central nitrogen functionality which reduces the flexibility of the ligand. Using molecular modeling, we have explored this flexibility and found that the planar nitrogen does not interfere with the S2 pocket steric restrictions and that the experimental potency of the described inhibitors is higher compared to that of the C analogues. However, the interference is different in the case of the P1 substituent where benzamidoxime moiety of molecules **6a**–**d** has more accessible conformers than its carbon analogues **6aC**–**6dC**.

Further optimization of the ligands at the S1 pocket is under way in this laboratory.

Experimental

Chemistry

Melting points were determined on a Reichter hot stage microscope and are uncorrected. ^{1}H NMR spectra were recorded on a Bruker Avance DPX_{300} spectrometer or on a Varian INOVA 600 MHz spectrometer. The proton chemical shifts of **6a**–**d** were assigned following standard procedures using homonuclear DQF-COSY, TOCSY, and NOESY experiments and are reported in δ (ppm) relative to tetramethylsilane. In NMR assignments the symbol 'Pip' refers to piperidine or in compounds **4d**, **5d** and **6d** to the hexahydro-1H-azepine ring, 'Ar' to phenyl and 'Nph' to naphthalene ring. The IR spectra were recorded on a Perkin-Elmer FTIR 1600 spectrophotometer. Mass spectroscopy was performed on Varian-MAT 311A mass spectrometer. Elemental analyses for all new compounds were performed on a Perkin-Elmer 240 C C, H, N analyzer. All solvents and reagents used in the syntheses were of commercial synthetic grade and when required were further purified and dried by standard methods. All reactions with air- or moisture-sensitive reactants were carried out under an argon atmosphere. Reagent abreviations: DIEA stands for *N,N*-diisopropylethylamine.

***tert*-Butyl-2-(4-cyanobenzylidene)hydrazinecarboxylate (2).** 4-Cyanobenzaldehyde (5.11 g, 39.0 mmol) **1** suspended in EtOH (100 mL) was added to a stirred solution of *tert*-butylcarbazate (5.29 g, 40.0 mmol) in EtOH. The mixture was heated at reflux temperature and after 4 h the EtOH was partially evaporated in vacuo. Water (100 mL) was added and the precipitated product was collected by filtration and washed with diethylether to give 9.12 g (95%) of the title compound **2** as a white solid. Mp 158–160 °C (lit. 154–158 °C);[34] IR (KBr) 3297, 2996, 2227, 1701, 1531, 1459, 1374, 1258, 1149, 1058, 946, 833, 772, 610 cm^{-1}; 300.15 MHz ^{1}H NMR ($CDCl_3$): 1.56 (s, 9H, Boc-H), 7.65 (d, J = 8.3 Hz, 2H, Ar–$H^{2,3}$), 7.77 (d, J = 8.3 Hz, 2H, Ar–$H^{5,6}$), 7.93 (s, 1H, CH), 8.13 (s, 1H, NH); FAB-MS: MH^+ = 246.

***tert*-Butyl 2-(4-cyanobenzyl)hydrazinecarboxylate (3).** *tert*-Butyl 2-(4-cyanobenzylidene) hydrazinecarboxylate **2** (14.88 g, 60.7 mmol) was dissolved in MeOH (250 mL) and 10% Pd/C (1.49 g, 10 w/w%) was added. The mixture was hydrogenated for 6 h. The catalyst was filtered off and the filtrate was evaporated in vacuo to yield oily **3** (14.52 g, 97%) which crystallized overnight. Mp 58–64 °C (lit. 66–69 °C);[34] IR (KBr) 3366, 3236, 2984, 2932, 2225, 1685, 1484, 1368, 1284, 1166, 1023, 818 cm^{-1}; 300.15 MHz ^{1}H NMR ($CDCl_3$): 1.45 (s, 9H, Boc-H), 4.05 (d, J = 4.5 Hz, 2H, CH_2), 4.31 (br s, 1H, NH), 6.18 (br s, 1H, NH), 7.46 (d, J = 8.3 Hz, 2H, Ar–$H^{2,6}$), 7.61 (d, J = 8.3 Hz, 2H, Ar–$H^{3,5}$); FAB-MS: MH^+ = 248.

***tert*-Butyl 2-(4-cyanobenzyl)-2-(1-piperidinylcarbonyl)-hydrazinecarboxylate (4a).** Triphosgene (6.98 g, 23.49 mmol) was dissolved in CH_2Cl_2 (40 mL) and a mixture of *tert*-butyl 2-(4-cyanobenzyl)hydrazinecarboxilate **3** (11.64 g, 47.06 mmol) and DIEA (12.28 mL, 70.59 mmol) in CH_2Cl_2 (80 mL) was slowly added to the stirred solution of triphosgene over a period of 30 min. After a further 5 min of stirring, a solution of piperidine (4.64 mL, 46.94 mmol) and DIEA (12.28 mL, 70.59 mmol) in CH_2Cl_2 (80 mL) was added in one lot. The reaction mixture was stirred for 30 min, evaporated to dryness, diluted with EtOAc (100 mL), washed with 10% aqueous citric acid 50 mL), 10% aqueous $NaHCO_3$ (50 mL) and saline solution(50 mL), dried and evaporated under reduced pressure to give oily **4a**. The product was crystallized from diethylether as white crystals (6.59 g, 42%). Mp 50–55 °C; IR (KBr) 3294, 2942, 2229, 1730, 1638, 1519 cm^{-1}; 300.15 MHz ^{1}H NMR (DMSO-d_6): 1.28–1.60 (m, 6H, Pip–$H^{3,4,5}$), 1.37 (s, 9H, Boc), 2.97–3.20 (m, 4H, Pip–$H^{2,6}$), 4.45 (br s, 2H, CH_2), 7.50 (d, J = 8.3 Hz, 2H, Ar–$H^{2,6}$), 7.78 (d, J = 8.3 Hz, 2H, Ar–$H^{3,5}$), 9.27 (s, 1H, NH); FAB-MS: MH^+ = 359. Anal. calcd for $C_{19}H_{26}N_4O_3$: C, 63.67; H, 7.31; N, 15.63; found: C, 63.29; H, 6.95; N, 15.34.

4b, **4c** and **4d** were prepared by the same methods described above for the synthesis of **4a** using appropriate starting compounds.

***tert*-Butyl 2-(4-cyanobenzyl)-2-[(2-methyl-1-piperidinyl)-carbonyl]hydrazine carboxylate (4b).** Yield: 3.99 g (38%). Mp 43–47 °C; IR (KBr) 3284, 2978, 2229, 1727, 1639 cm^{-1}; 300.15 MHz ^{1}H NMR (DMSO-d_6): 1.10 (d, J = 6.8 Hz, 3H, CH_3), 1.36 (s, 9H, Boc), 1.36–1.53 (m, 1H, Pip–H) 1.48–1.53 (m, 5H, Pip–H), 2.88 (t, J = 12.4 Hz, 1H, Pip–H), 3.50–3.59 (m, 1H, Pip–H), 3.99–4.20 (m, 1H, Pip–H), 4.46 (br s, 2H, CH_2), 7.50 (d, J = 8.3 Hz, 2H, Ar–$H^{2,6}$), 7.78 (d, J = 8.3 Hz, 2H, Ar–$H^{3,5}$), 9.27 (s, 1H, NH); FAB-MS: MH^+ = 373. Anal. calcd for C_{20} H_{28} N_4 O_3: C, 64.49; H, 7.58; N, 15.04; found C, 64.06; H, 7.64; N, 14.85.

***tert*-Butyl 2-(4-cyanobenzyl)-2-[(4-methyl-1 piperidinyl)-carbonyl]hydrazine carboxylate (4c).** Yield: 3.67 g (81%). Mp 55–58 °C; IR (KBr) 3284, 2977, 2228, 1728, 1636 cm^{-1}; 300.15 MHz ^{1}H NMR ($CDCl_3$): 0.96 (d, J = 6.4 Hz, 3H, CH_3), 0.90–1.05 (m, 2H, Pip–$H^{3,5}$), 1.45 (s, 9H, Boc), 1.45–1.60 (m, 4H, Pip-$H^{3',5'}$), 2.60–2.75 (m, 2H, Pip–$H^{2,6}$), 3.70–3.85(m, 2H, Pip–$H^{2',6'}$), 4.52 (br s,

2H, CH_2), 7.48 (d, $J=8.3$ Hz, 2H, Ar–$H^{2,6}$), 7.61 (d, $J=8.3$ Hz, 2H, Ar-$H^{3,5}$), 9.32 (s, 1H, NH); FAB-MS: $MH^+=373$. Anal. calcd for $C_{20}H_{28}N_4O_3$: C, 64.49; H, 7.58; N, 15.04; found: C, 64.89; H, 7.66; N, 15.30.

***tert*-butyl 2-(1-azepanylcarbonyl)-2-(4-cyanobenzyl)hydrazinecarboxylate (4d).** Yield: 1.58 g, (35%). Mp 136–141 °C; IR (KBr) 3287, 2925, 2223, 1726, 1634 cm^{-1}; 300.15 MHz ^1H NMR ($CDCl_3$): 1.44 (s, 9H, Boc), 1.51–1.62 (m, 4H, Pip–$H^{4,5}$), 1.65–1.78 (m, 4H, Pip–$H^{3,6}$), 3.30–3.49 (m, 4H, Pip–$H^{2,7}$), 4.53 (s, 2H, CH_2), 6.24 (br s, 1H, NH), 7.51 (d, $J=8.3$ Hz, 2H, Ar–$H^{2,6}$), 7.63 (d, $J=8.3$ Hz, 2H, Ar–$H^{3,5}$); FAB-MS: $MH^+=373$. Anal. calcd for $C_{20}H_{28}N_4O_3$: C, 64.49; H, 7.58; N, 15.04; found: C, 64.79; H, 7.56; N, 15.34.

***N*′-(4-Cyanobenzyl)-*N*-(1-piperidinylcarbonyl)-2-naphthalenesulfonylhydrazide (5a).** HCl gas was bubbled for 45 min through a solution of *tert*-butyl 2-(4-cyanobenzyl)-2-(1-piperidinylcarbonyl)hydrazinecarboxylate **4a** (1.38 g, 3.86 mmol) in AcOH (15 mL) at room temperature. AcOH was evaporated in vacuo to yield oily 2-(4-cyanobenzyl)-2-(1-piperidinylcarbonyl)hydrazinum chloride (1.04 g, 3.53 mmol). To a solution of this compound in CH_2Cl_2 (50 mL) cooled to 0 °C were added DIEA (1.23 mL, 7.06 mmol) and naphthalene-2-sulphonylchloride (0.80 g, 3.53 mmol). The mixture was stirred overnight at rt and concentrated in vacuo. The residue was dissolved in EtOAc (100 mL) and washed with H_2O (50 mL), 1 M HCl (50 mL) and brine (50 mL). The organic phase was dried over Na_2SO_4. After evaporation of the solvent under reduced pressure, the product was crystallized from diethylether as white crystals (0.58 g, 33%). Mp 155–157 °C; IR (KBr) 2940, 2233, 1801, 1630 cm^{-1}; 300.15 MHz ^1H NMR (DMSO-d_6): 1.04–1.45 (m, 8H, Pip–$H^{3,4,5}$), 2.90–3.20 (m, 4H, Pip-$H^{2,6}$), 4.29 (br d, 2H, CH_2), 7.16 (d, 2H, $J=8.6$ Hz, Ar–$H^{2,6}$), 7.65–7.77 (m, 5H, Ar–$H^{3,5}$ and Nph–$H^{3,6,7}$), 8.05–8.17 (m, 3H, Nph–$H^{4,5,8}$), 8.43 (s, 1H, Nph–H^1), 9.59 (s, 1H, NH); FAB-MS: $MH^+=449$. Anal. calcd for $C_{24}H_{24}N_4O_3S$: C, 64.27; H, 5.39; N, 12.49; found: C, 63.98; H, 5.19; N, 12.49.

5b, **5c** and **5d** were prepared by the same methods described above for the synthesis of **5a** using appropriate starting compounds.

***N*′-(4-Cyanobenzyl)-*N*′-[(2-methyl-1-piperidinyl)carbonyl]-2 naphthalenesulfonohydrazide (5b).** Yield: 0.50 g (27%). Mp 128–132 °C; IR (KBr) 3240, 2950, 2228, 1652 cm^{-1}; 300.15 MHz ^1H NMR (DMSO-d_6): 0.35–0.54 (m, 2H, Pip–$H^{3,3',5,5'}$), 0.60–0.90 (m, 2H, Pip-$H^{3,3',5,5'}$), 1.15–1.50 (m, 5H, Pip–$H^{4,4'}$ and CH_3), 2.55–2.70, 2.75–2.95, 3.34–3.36 (m, 2H, Pip–$H^{6,6'}$), 3.65–3.80, 3.85–4.15 (m, 1H, Pip–$H^{2,2'}$), 4.33 (br s, 2H, CH_2), 7.36 (d, 2H, $J=8.3$ Hz, Ar–$H^{2,6}$), 7.67–7.75 (m, 5H, Ar–$H^{3,5}$ and Nph–$H^{3,6,7}$), 8.02–8.16 (m, 3H, Nph–$H^{4,5,8}$), 8.42 (s, 1H, Nph–H^1), 9.44 (br s, 1H, NH) (two sets of signals); FAB-MS: $MH^+=463$. Anal. calcd for $C_{25}H_{26}N_4O_3S$: C, 64.91; H, 5.67; N, 12.11; found: C, 65.17; H, 5.70; N, 12.15.

***N*′-(4-Cyanobenzyl)-*N*′-[(4-methyl-1-piperidinyl)carbonyl]-2-naphthalenesulfonohydrazide (5c).** Yield: 0.43 g (22%). Mp 148–151 °C; IR (KBr) 3191, 3054, 2913, 2224, 1686 cm^{-1}; 300.15 MHz ^1H NMR (DMSO-d_6): 0.10–0.35 (m, 2H, Pip–$H^{3,3',5,5'}$), 0.47 (d, 3H, $J=6.0$ Hz, CH_3), 1.22–1.26 (m, 3H, Pip–$H^{3,3',4,4',5,5'}$), 2.30–2.45 (m, 1H, Pip–$H^{2,2'}$), 2.65–2.80 (m, 1H, Pip–$H^{6,6'}$), 3.45–3.65 (m, 2H, Pip–$H^{2,2',\ 6,6'}$), 4,38 (br d, 2H, CH_2), 7.34 (d, 2H, $J=8.3$, Ar–$H^{2,6}$), 7.64–7.80 (m, 5H, Ar–$H^{3,5}$ and Nph–$H^{3,6,7}$), 8.02–8.18 (m, 3H, Nph–$H^{4,5,8}$), 8.42 (s, 1H, Nph–H^1), 9.55 (s, 1H, NH) (two sets of signals); FAB-MS: $MH^+=463$. Anal. calcd for C_{25} H_{26} N_4 O_3 S: C, 64.91; H, 5.67; N, 12.11; found: C, 64.86; H, 5.58; N, 12.17.

***N*′-(1-Azepanylcarbonyl)-*N*′-(4-cyanobenzyl)-2-naphthalenesulfonohydrazide (5d).** Yield: 0.26 g (22%). Mp 192–194 °C; IR (KBr) 3195, 2931, 2221, 1676 cm^{-1}; 300.15 MHz ^1H NMR (DMSO-d_6): 0.63–1.48 (m, 8H, Pip–$H^{3,4,5,6}$), 3.18 (m, 4H, Pip–$H^{2,7}$), 4.35 (br d, 2H, CH_2), 7.31 (d, $J=8.3$ Hz, 2H, Ar–$H^{2,6}$), 7.55 (d, $J=8.3$ Hz, 2H, Ar–$H^{3,5}$), 7.64 (m, 1H, Nph–H^7), 7.69 (m, 1H, Nph–H^6), 7.77 (d, 1H, $J=7.8$, Nph–H^3), 8.01 (d, 1H, $J=7.8$, Nph–H^5), 8.05 (d, 1H, $J=7.8$, Nph–H^4), 8.13 (d, 1H, $J=7.8$, Nph–H^8), 8.45 (s, 1H, Nph–H^1), 9.35 (s, 1H, NH); FAB-MS: $MH^+=463$. Anal. calcd for $C_{25}H_{26}N_4O_3S$: C, 64.91; H, 5.67; N, 12.11; found: C, 64.93; H, 5.71; N, 12.26.

***N*′-Hydroxy-4-{[2-(2-naphtylsulfonyl)-1-(1-piperidinylcarbonyl)hydrazino]methyl}benzenecarboximidamide (6a).** NH_2OH (0.54 g, 16.4 mmol) was added to the solution of *N*′-(4-cyanobenzyl)-*N*-(1-piperidinylcarbonyl)-2-naphthalenesulfonylhydrazide **5a** (3.68 g, 8.20 mmol) in EtOH (100 mL). The mixture was heated at reflux temperature overnight and evaporated under reduced pressure to yield white foam **6a**. Product was purified by column chromatography on silica gel ($CHCl_3$/MeOH, 50:1). Yield: 1.49 g (38%). Mp 194–197 °C; IR (KBr) 3383, 1660, 1427, 1335 cm^{-1}; 600 MHz ^1H NMR (DMSO-d_6): 1.03 (br s, 4H, Pip–$H^{3,5}$), 1.24 (m, 2H, $J=5.75$ Hz, Pip–H^4), 2.93 (br s, 2H, Pip–$H^{2,6}$), 3.06 (br s, 2H, Pip–$H^{2',6'}$), 4.18 (br s, 1H, CH_21), 4.38 (br s, 1H, CH_22), 5.78 (s, 2H, NH_2), 7.16 (d, 2H, $J=8.2$ Hz, Ar–$H^{2,6}$), 7.58 (d, 2H, $J=8.2$ Hz, Ar–$H^{3,5}$), 7.68 (dd, 1H, $J=8.0$, Nph–H^7), 7.71 (dd, 1H, $J=8.0$ Hz, Nph–H^6), 7.77 (d, 1H, $J=8.6$ Hz, Nph–H^3), 8.04 (d, 1H, $J=8.0$ Hz, Nph–H^5), 8.09 (d, 1H, $J=8.0$ Hz, Nph–H^4), 8.16 (d, 1H, $J=8.0$ Hz, Nph–H^8), 8.46 (s, 1H, Nph–H^1), 9.41 (s, 1H, NH), 9.61 (s, 1H, OH); FAB-MS: $MH^+=482$. Anal. calcd for $C_{24}H_{27}N_5O_4S$: C, 59.86; H, 5.65; N, 14.54; found C, 59.49; H, 5.33; N, 14.25.

The following compounds were prepared by the same methods described above for the synthesis of **6a**, using appropriate starting compounds.

***N*′-Hydroxy-4-{[1-[(2-methyl-1-piperidinyl)carbonyl]-2-(2-naphthylsulfonyl)hydrazino]methyl}benzenecarboximidamide (6b).** Yield: 0.15 g (47%). Mp 174–176 °C; IR (KBr) 3369, 2936, 1647 cm^{-1}; 600 MHz ^1H NMR (DMSO-d_6): 0.23 and 0.69 (br s, 3H, CH_3), 0.54 and 1.01 (br s, 1H, Pip–H^5), 0.74 and 1.03 (br s, 1H, Pip–H^3), 1.12 and 1.14 (br s, 1H, Pip–$H^{3'}$), 1.26 and 1.31 (br s, 1H, Pip–H^4), 1.32 and 1.41 (br s, 1H, Pip–$H^{5'}$), 2.52

and 2.86 (br s, 1H, Pip–H^6), 3.34 and 3.52 (br s, 1H, Pip–$H^{6'}$), 3.57 and 3.87 (br s, 1H, Pip–$H^{2'}$), 4.11 and 4.19 (br s, 1H, $CH_2$2), 3.30 (br s, 1H, $CH_2$1), 5.85 (s, 2H, NH_2), 7.13 and 7.15 (d, 1H, J = 8.2 Hz, Ar–$H^{2,6}$), 7.49 and 7.51 (d, 1H, J = 8.2 Hz, Ar–$H^{3,5}$), 7.64 (dd, 1H, Nph–H^7), 7.78 (dd, 1H, Nph–H^6), 7.70 (d, 1H, Nph–H^3), 7.97 (d, 1H, Nph–H^5), 8.03 (d, 1H, Nph–H^4), 8.07 (d, 1H, Nph–H^8), 8.36 and 8.37 (s, 1H, Nph–H^1), 9.16 and 9.39 (br s, 1H, NH), 9.62 (s, 1H, OH); FAB-MS: M^+ = 496. Anal. calcd for $C_{25}H_{29}N_5O_4S$: C, 60.59; H, 5.90; N, 14.13; found: C, 60.27; H, 5.81; N, 13.91.

***N′*-Hydroxy-4-{[1-[(4-methyl-1-piperidinyl)carbonyl]-2-(2-naphthylsulfonyl)hydrazino]methyl}benzenecarboximidamide (6c).** Yield: 0.26 g (56%). Mp 195–197 °C; IR (KBr) 3414, 2947, 1654 cm^{-1}; 600 MHz ^{1}H NMR (DMSO-d_6): 0.06 (br s, 1H, Pip–H^5), 0.25 (br s, 1H, Pip–H^3), 0.43 (s, 3H, CH_3), 1.20 (br s, 3H, Pip–$H^{3',4,5'}$), 2.35 (br s, 1H, Pip–$H^{2'}$), 2.65 (br s, 1H, Pip–$H^{6'}$), 3.50 (br s, 1H, Pip–H^6), 3.55 (br s, 1H, Pip–H^2), 4.22 (br s, 1H, $CH_2$2), 4.39 (br s, 1H, $CH_2$1), 5.78 (s, 2H, NH_2), 7.16 and 7.23 (d, 1H, J = 8.2 Hz, Ar–$H^{2,6}$), 7.59 and 7.79 (d, 1H, J = 8.2 Hz, Ar–$H^{3,5}$), 7.66 (dd, 1H, J = 8.0, Nph–H^7), 7.71 (dd, 1H, J = 8.0, Nph–H^6), 7.77 (d, 1H, J = 8.0, Nph–H^3), 8.03 (d, 1H, J = 8.0 Hz, Nph–H^5), 8.07 (d, 1H, J = 8.0 Hz, Nph–H^4), 8.14 (d, 1H, J = 8.0 Hz, Nph–H^8), 8.45 (s, 1H, Nph–H^1), 9.39 and 9.46 (br s, 1H, NH), 9.62 (s, 1H, OH); FAB-MS: MH^+ = 496. Anal. calcd for $C_{25}H_{29}N_5O_4S$: C, 60.59; H, 5.90; N, 14.13; found: C, 60.18; H, 5.93; N, 13.65.

4-{[1-(1-Azepanylcarbonyl)-2-(2-naphthylsulfonyl)hydrazino]methyl}-*N′*-hydroxybenzenecarboximidamide (6d). Yield: 0.07 g (57%). Mp 193–195 °C; IR (KBr) 3402, 3255, 2921, 1648 cm^{-1}; 600 MHz ^{1}H NMR (DMSO-d_6): 0.65 (br s, 2H, Pip–$H^{4,5}$), 1.00 (br s, 2H, Pip–$H^{4',5'}$), 1.14 (br s, 2H, Pip–$H^{3,6}$), 1.32 (br s, 2H, Pip–$H^{3',6'}$), 2.97 (br s, 2H, Pip–$H^{2,7}$), 3.13 (br s, 2H, Pip–$H^{2',7'}$), 4.17 (s, 1H, $CH_2$1), 4.41 (s, 1H, $CH_2$2), 5.77 (s, 2H, NH_2), 7.16 (d, 2H, J = 8.1 Hz, Ar–$H^{2,6}$), 7.58 (d, 2H, J = 8.1 Hz, Ar–$H^{3,5}$), 7.65 (dd, 1H, J = 8.1 Hz, Nph–H^7), 7.69 (dd, 1H, J = 8.1 Hz, Nph–H^6), 7.77 (d, 1H, J = 8.7 Hz, Nph–H^3), 8.01 (d, 1H, J = 8.1 Hz, Nph–H^5), 8.05 (d, 1H, J = 8.1 Hz, Nph–H^4), 8.13 (d, 1H, J = 8.1 Hz, Nph–H^8), 8.45 (s, 1H, Nph–H^1), 9.35 (s, 1H, NH), 9.60 (s, 1H, OH); FAB-MS: MH^+ = 466. Anal. calcd for $C_{25}H_{29}N_5O_4S$: C, 60.59; H, 5.90; N, 14.13; found: C, 60.27; H, 5.78; N, 14.26.

Molecular modelling

Molecular simulations were performed on a Silicon Graphics workstation using Insight/Discover programs.[35,36] Our starting point was X-ray structural data of the human α thrombin–BMS189090 inhibitor complex. Structural data for several other complexes of human α thrombin with the inhibitors BMS186282, PPACK, modified PPACK, *p*-amidinophenylpyruvate and Ac-D-Phe-Pro-boroarg-OH were also used in the following manner. By superimposing 21 amino acids from the active site onto corresponding amino acids of the BMS-189090 inhibitor complex, we found that the position of various inhibitors was restricted to the S1, S2 and S3 pocket. The benzamidoxime group was positioned in the S1 site, the piperidine or hexahydro-1H-azepine ring in the S2 and the naphthalene-2-sulfonyl group in the S3. As RMS values of the superimposed active sites of proteins were in the range of 1.07–1.28 Å, we concluded that the binding of different inhibitors does not change the conformation of the active site to the extent that would preclude the techniques we used. A sphere of water molecules (2R = 40 Å) was added around the inhibitor in order to simulate the effects of solvent. Minimal energies were computed for these complexes using the Discover program until the maximal gradients were lower than 0.001 kcal/molA. After minimization of these complexes, we performed a systematic conformational analysis of the flexible angles in the inhibitor backbone. Bearing in mind that the conformational space of the inhibitors is restricted by three specificity pockets (S1, S2 and S3), our search was aimed at determining the differential flexibility of the aza versus the α-CH structural elements in the enzyme active site. Ten-degree steps rotations around angles α0–α4 (Fig. 5a and b) resulted in 37 conformations for these rotations around a single bond and in 1369 conformations for rotations around two subsequent bonds. The potential energy of the 37 and 1369 inhibitor–enzyme complexes was calculated. Since the active site of the inhibitor was kept rigid, the majority of conformations showed repulsion contacts and thus high positive energy values. The conformations with favorable (negative) energy values were numbered, and are presented in Table 1. This procedure was also performed with the carbon analogues.

Solution structure determination by 2-D NMR

Nuclear magnetic resonance. NMR spectra were recorded on Varian INOVA 600 MHz in DMSO-d_6 at 298 K and in mixture of DMSO-d_6/H_2O (80%/20%) H_2O at 273 K. The sample concentrations were 10 mM. The DQF-COSY,[37] WET-DQF-COSY and WG-NOESY were performed using gradients. The TOCSY,[38,39] NOESY[40] and ROESY experiments were recorded using standard pulse sequences in the phase-sensitive mode. The TOCSY spectra were recorded with a MLEV-17[39] mixing sequence of 60 ms and a 10-kHz spin-lock field strength. NOESY spectra of **6a** were measured at four different mixing times 75, 150, 300, and 450 ms. For the other compounds, a mixing time of 75 ms was used. The ^{1}H sweep width was from 6800 to 8000 Hz for different compounds. Typically, the homonuclear proton spectra were acquired with 4096 data points in t_2, 16–32 scans, 256–512 complex points in t_1, and a relaxation delay of 1–1.5 s. Data were processed and analyzed with the FELIX software package from Biosym Technologies. Spectra were zero-filled two times and apodizied with a squared sine bell function shifted by π/2 in both dimensions.

The proton–proton distances were calculated from the NOESY spectra measured at 75 ms using the two-spin approximation and the integrated intensity of a geminal pair of protons assumed to have a distance of 1.78 Å. All compounds are in the positive NOE regime when

studied in DMSO at 298 K and in negative NOE regime when studied in mixture of DMSO/H_2O at 273 K The ROESY spectra of LK-632 in DMSO display significant spin-diffusion effects, which were identified by the examination of ROESY spectra collected at different mixing times (75, 150, 200, and 250 ms). Based on this the mixing time of 75 ms was chosen for determination of distances of other compounds. A pseudo-atom correction was added for the methyl and methylene groups and a $\pm 10\%$ correction were applied to the distance in order to produce the upper and lower limit constraints.

Molecular dynamics. MD simulations were performed using DISCOVER (Consistent Valence Force Field) and INSIGHT II software from Biosym Technologies. Several simulations with different starting structures for each of the compounds were carried out in DMSO.[30] The molecule with all atoms treated explicitly was centred in a cubic box ($x=y=z=40$ Å) using three-dimensional periodic boundary conditions. The dielectric constant was set to 1.0. Neighbor lists for calculation of non-bonded interactions were updated every 10 fs within a radius of 14 Å. The actual calculation of non-bonded interactions was carried out up to a radius of 12 Å without the use of switching functions. A time step of 1 fs was employed for the MD simulation. The simulation protocol consisted of two minimization cycles (steepest descent and conjugate gradients), first with the solute fixed and then with all the atoms allowed to move freely. The convergence criterion was 1 kcal $Å^{-1}$. The initial MD phase of the calculation involved a gradual heating, starting from 100 and then increasing to 150, 200, 250 and finally to 300 K in steps of 0.5, 0.5, 5, 1, and 5 ps, respectively, each by direct scaling of the velocities. The NMR-derived distance restraints with a force constant of 10 kcal mol^{-1} $Å^{-1}$ were applied during the entire simulation. Configurations were saved every 1 ps for another 200 ps of dynamics. The last 100 ps of the trajectory was used for analysis of NOE distance violations and dihedral angles.

Enzyme assay

Spectrophotometric enzyme tests were run in microtiter plates in a final volume of 125 μL using the following conditions: the inhibition of factor VIIa was tested with TF/FVIIa/Ca^{2+} at a final concentration of 15 nM/5 nM/5 mM with the substrate Cromozym-tPA at 500 μM f.c. Thrombin was tested at 1 nM with the substrate S-2366 at 200 μM f.c. Factor Xa was tested at 3 nM with S-2222 at 200 nM. Trypsin was tested at 6 nM using the substrate S-2251 at 200 nM. The reaction kinetics between enzymes and substrates were linear both with time and the concentration of the enzyme chosen. Inhibitors were dissolved in DMSO and tested at 100 μM as the highest concentration. Inhibitors were diluted using HNPT buffer consisting of HEPES 100 mM, NaCl 140 mM, PEG 6000 0.1% and Tween 80 0.02%, pH 7.8. Full concentration dose–response curves were run for inhibitors showing inhibition $>50\%$ for any one enzyme at 100 μM. Apparent K_i were calculated according to Cheng and Prusoff[41] based on the IC_{50} and the respective K_m, which had been previously determined [$K_i = IC_{50}/(1 + S/K_m)$]. The K_m for the substrates used were determined under the conditions of the test with at least five substrate concentrations ranging from 0.5 to 15 times K_m (Lottenberg et al.)[42] according to Eadie.[43] The K_m was 1132 μM for Chromozym-tPA, 108 μM for S-2366, 613 μM for S-2222 and 430 μM for S-2251.

Acknowledgements

The authors are grateful to Ministry of Science and Technology of Republic Slovenia for partial financial support (grant No. J1-8889) and Lek, d.d. for support of T.S. and U.U. We cordially thank Ms. Charlotte Taft for linguistic help with the manuscript.

References and Notes

1. Stryer, L. *Biochemistry*, 4th ed.; W. H. Freeman: New York, 1995; pp 252–258.
2. Mutschler, E. *Arzneimittelwirkungen: Lehrbuch der Pharmakologie und Toxikologie: mit einf"hrenden Kapiteln in die Anatomie, Physiologie und Patophysiologie*, 7th ed.; Wissenschaftliche Verlagsgellschaft: Stuttgart, 1996; pp 413–414, 425–430.
3. (a) Hirsh, J.; Fuster, V. *Circulation* **1994**, *89*, 1449. (b) Hirsh, J.; Fuster, V. *Circulation* **1994**, *89*, 1469.
4. Taparelli, C.; Metternich, R.; Erhardt, C.; Cook, N. S. *TIPS* **1993**, *14*, 366.
5. Kimball, S. D. *Curr. Pharm. Design* **1995**, *1*, 441.
6. Ripka, W. C.; Vlasuk, G. P. *Ann. Rep. Med. Chem.* **1997**, *32*, 71.
7. Wiley, M. R.; Fisher, M. J. *Exp. Opin. Ther. Patents* **1997**, *7*, 1265.
8. Sanderson, P. E. J.; Naylor-Olsen, A. M. *Current Med. Chem.* **1998**, *5*, 289.
9. Rewinkel, J. B. M.; Adang, A. E. P. *Curr. Pharm. Design* **1999**, *5*, 1043.
10. Menear, K. *Current Med. Chem.* **1998**, *5*, 457.
11. Renatus, M.; Bode, W.; Huber, R.; Stuerzebecher, J.; Stubbs, M. *J. Med. Chem.* **1998**, *41*, 5445.
12. Gardell, S. J.; Sanderson, P. E. J. *Coron. Artery Dis.* **1998**, *9*, 75.
13. Wagner, J.; Kallen, J.; Ehrhardt, C.; Evenou, J.-P.; Wagner, D. *J. Med. Chem.* **1998**, *41*, 3664.
14. Misra, R. N.; Kelly, Y. F.; Brown, B. R.; Roberts, D. G. M.; Chong, S.; Seiler, S. M. *Biorg. Med. Chem. Lett.* **1994**, *4*, 2165.
15. Balasubramanian, B. N. *Bioorg. Med. Chem.* **1995**, *3*, 999.
16. Kikomoto, R.; Tonomura, S.; Hara, H.; Ninomya, K.; Maruyama, A.; Sugano, M.; Tamao, Y. *Biochem. Biophys. Res. Commun.* **1981**, *101*, 440.
17. Kikumoto, R.; Tamao, Y.; Tezuka, T.; Tonomura, S.; Hara, H.; Ninomiya, K.; Hijikata, A.; Okamoto, S. *Biochemistry* **1984**, *23*, 85.
18. Kim, S.; Hwang, S. Y.; Kim, Y. K.; Yun, M.; Oh, Y. S. *Bioorg. Med. Chem. Lett.* **1997**, *7*, 769.
19. Oh, Y. S.; Yun, M.; Hwang, S. Y.; Hong, S.; Shin, Y.; Lee, K.; Yoon, K. H.; Yoo, Y. J.; Kim, D. S.; Lee, S. H.; Lee, Y. H.; Park, H. D.; Lee, C. H.; Lee, S. K.; Kim, S. *Bioorg. Med. Chem. Lett.* **1998**, *8*, 631.
20. Lee, K.; Hwang, S. Y.; Hong, S.; Hong, C. Y.; Lee, C.-S.; Shin, Y.; Kim, S.; Yun, M.; Yoo, Y. J.; Kang, M.; Oh, Y. S. *Bioorg. Med. Chem. Lett.* **1998**, *6*, 869.

21. (a) Danilewitcz, J. C.; Kobylecki, R. J.; Ellis, D. International Patent Aplication WO 9513274, 1995. (b) Allen, M.; Abel, S. M.; Barber, C. G.; Cussans, N. J.; Danilewicz, J. C.; Ellis, D.; Hawkeswood, E.; Herron, M.; Holland, S.; Fox, D. N. A.; James, K.; Kobylecki, R. J.; Overington, J. P.; Pandit, J.; Parmar, H.; Powling, M. J.; Rance, D. J.; Taylor, W.; Shepperson, N. B. 215th ACS National Meeting, 1998, Dallas, TX; Abstract MEDI 64.
22. Gante, J. *Synthesis* **1989**, *259*, 405.
23. Gante, J. *Angew. Chem.* **1994**, *106*, 1780.
24. Powers, J. C.; Gupton, B. F. *Methods Enzymol.* **1977**, *46*, 208.
25. Kurtz, A. N.; Niemann, C. *J. Org. Chem.* **1961**, *26*, 1843.
26. Dorn, C. P.; Zimmerman, M.; Yang, S. S.; Yurewicz, E. C.; Ashe, B. M.; Frankshun, R.; Jones, H. *J. Med. Chem.* **1977**, *20*, 1464.
27. Spatola, A. F. *Chemistry and Biochemistry of Amino Acids, Peptides, and Proteins*; Weinstein, B., Ed.; Marcel Dekker: New York, 1983; pp 267–357.
28. Dutta, A. S.; Morley, J. S. *J. Chem. Soc., Perkin Trans. 1* **1976**, 244.
29. Eckert, H.; Foster, B. *Angew. Chem. Int. Ed.* **1987**, *26*, 894.
30. Mierke, D. F.; Kessler, H. *J. Am. Chem. Soc.* **1991**, *113*, 9466.
31. Malley, F. M.; Tabernero, L.; Chang, C. Y.; Ohringer, S. L.; Roberts, D. G. M.; Das, J.; Sack, J. S. *Protein Sci.* **1996**, *5*, 221.
32. Bauer, M.; Brandstetter, H.; Turk, D.; Stuerzebecher, J.; Bode, W. *Semin. Throm. Hemos.* **1993**, *19*, 352.
33. Pearse, G. A., Jr.; Pflaum, R. T. *J. Am. Chem. Soc.* **1959**, *81*, 6505.
34. Fässler, A.; Bold, G.; Capraro, H. G.; Cozens, R.; Mestan, J.; Poncioni, B.; Rösel, J.; Titelnot-Blomley, M.; Lang, M. *J. Med. Chem.* **1996**, *39*, 3203.
35. *InsightII Version 97.0*; MSI Inc.: San Diego, USA, 1997.
36. *Discover, Version 95.0*; MSI Inc.: San Diego, USA, 1995.
37. Rance, M.; Sorensen, O. W.; Bodenhausen, G.; Wagner, G.; Ernst, R. R.; Wütrich, K. *Biochem. Biophys. Res. Commun.* **1983**, *117*, 479.
38. Braunschweiler, L.; Ernst, R. R. *J. Magn. Reson.* **1983**, *53*, 521.
39. Bax, A.; Davis, D. G. *J. Magn. Reson.* **1985**, *65*, 355.
40. Jeener, J.; Meier, B. H.; Bachmann, P.; Ernst, R. R. *J. Chem. Phys.* **1979**, *71*, 4546.
41. Cheng, Y. C.; Prusoff, W. H. *Biochem. Pharmacol.* **1973**, *22*, 3099.
42. Lottenberg, R.; Hall, J. A.; Blinder, M.; Binder, E. P.; Jackson, C. R. *Biochem. Biophys. Acta* **1983**, *742*, 539.
43. Eadie, G. S. *J. Biol. Chem.* **1942**, *146*, 85.